Fisheries Research 200 (2018) 93–103

Contents lists available at ScienceDirect

Fisheries Research

journal homepage: www.elsevier.com/locate/fishres

Extracting a time-varying climate-driven growth index from otoliths for use in stock assessment models

Qi Lee*, André E. Punt

School of Aquatic and Fishery Sciences, University of Washington, Box 355020, Seattle, WA, 98105, USA

ARTICLE INFO

Handled by George A. Rose

Keywords:
Growth variation
Environmental index
Climate change
Simulation testing
Otolith growth
Mixed effects model

ABSTRACT

Understanding the characteristics of individual growth is a critical component of population assessment. Most fisheries stock assessments assume constant values for each life history parameter, despite growing evidence that growth is variable at individual, temporal, and spatial scales. Otoliths contain important information pertaining to age and growth, among other things, and otolith increment data correlate with climate indices on a decadal scale. We expand on this concept to include individual- and year-level variation, and develop a nonlinear mixed-effects model to analyze otolith increment data. We then fit the model to otolith increment data for splitnose rockfish, and simulation-test the ability to precisely estimate year effects without bias. Generally, given a sample size of at least 50 otoliths, the model performs well at estimating year effects. With this method, species-specific indices of growth can be extracted from otolith increment data, and potentially be used in stock assessments to detect the effects of climate change on fish growth.

1. Introduction

Climate can have varying degrees of impact on a population depending on life history stage, and these impacts are often highly complex and difficult to isolate (Black, 2009). Understanding variability in life history characteristics in space and time also helps determine the most appropriate assessment model structure (Gertseva et al., 2010), although time-variation in biological rates adds complexity to the definition of management targets (Thorson et al., 2015). Estimating the growth of individual fish is important to stock assessment modelling, as growth is one component of the productivity of a stock. Currently, most stock assessments assume time-invariant mean growth rates (Lorenzen, 2016), even though there is an increasing number of studies that show that growth actually varies over time (e.g., Black, 2009; Stawitz et al., 2015; Thorson and Minte-Vera, 2016), particularly in response to environmental factors such as temperature and food availability (Brett, 1979; Weatherley, 1990).

Collecting long-term (multiple decades) growth data on marine fish populations is often a lengthy and costly process, which makes mechanistic understanding of growth drivers difficult, and indices of growth variation hard to obtain. Stawitz et al. (2015) describe a state-space Bayesian modelling approach that uses fishery-dependent and −independent data to detect the presence of growth variation. However, sampling procedures (such as selectivity) could potentially be confounded in the annual growth anomalies, as acknowledged by the authors. Measurement of annually-formed growth increments, using a method known as dendrochronology, has been proposed as an alternative to direct measurements for the reconstruction of time series of environmental variation in growth (Black et al., 2005; Strom et al., 2004; Weisberg, 1993). Dendrochronology may be costly and time-consuming (Stawitz et al., 2015), but represents a fishery-independent source of data as back-calculation would allow for observations for ages that are rarely sampled, perhaps due to gear selectivity (Ballagh et al., 2011; López-Abellán et al., 2008). Additionally, otoliths contain historical information about growth that would allow of reconstruction of growth time series potentially dating back to before size-at-age data were available (Begg et al., 2005).

In terrestrial forested ecosystems, tree ring data have been widely used to reconstruct various aspects of climate, disturbance, and community dynamics, and are accepted as a way to capture changes in the environment (e.g., measuring a species' sensitivity to climate). Similarly, bony fish are known to deposit annual rings on their otoliths, much like tree rings (Pannella, 1980). Studies have previously examined the application of dendrochronology techniques to reconstruct time series of ocean conditions (Black, 2009; Strom et al., 2004). Widths between each ring on otoliths of splitnose rockfish (*Sebastes diploproa*) were measured, and detrended using cubic splines and autoregressive models to remove any age-related trends in the data (Black et al., 2005). The resulting time series was averaged to create an environmental index for the species, which was then found to be strongly

* Corresponding author. Present address: Bren School of Environmental Science and Management, Marine Science Institute, University of California, Santa Barbara, CA, 93106, USA.
E-mail address: leeqi@uw.edu (Q. Lee).

https://doi.org/10.1016/j.fishres.2017.12.014
Received 10 July 2017; Received in revised form 16 December 2017; Accepted 26 December 2017
Available online 08 January 2018
0165-7836/

correlated with various productivity indicators in the California Current Ecosystem and other dendrochronology indices obtained from trees and other marine species in the area (Black, 2009). However, early years of growth data for each otolith − particularly critical in short-lived species (Weisberg et al., 2010) − were removed from the study to allow for better model fit, which could affect the strength of the relationship between growth and the environment, as well as the precision of the resulting indices.

Rather than the use of cubic splines by Black et al. (2005), fish growth is often described using a nonlinear model such as the von Bertalanffy growth curve (Essington et al., 2001; Von Bertalanffy, 1957). Mixed effects models − where fixed effects describe the entire population, and random effects are associated with randomly-selected experimental units within the population (Pinheiro and Bates, 2000) − are often used to describe incremental growth data, repeatedly measured on the same individuals over a period of time ("longitudinal data", Liang and Zeger, 1986; Zeger and Liang, 1986). This method originated from a study on bacon pigs (Wishart, 1938), and followed by studies on emus (Palmer et al., 1991), clams (Escati-Peñaloza et al., 2010), and tree rings (Xu et al., 2014). Bayesian hierarchical von Bertalanffy growth curves have been used in meta-analyses to model overall fish length across similar species (Helser et al., 2007) and across geographic environments (Helser and Lai, 2004). They have also been used in tag-recapture studies on fish growth (e.g., Eveson et al., 2015; Zhang et al., 2009; Zhu et al., 2016), but, as mentioned previously, these data might not be readily available for many species. Pilling et al. (2002) fit a random effects von Bertalanffy growth model to length-at-age information back-calculated from otolith increment data for tropical emperor, *Lethrinus mahsena*, specifically incorporating individual (but not annual) growth variability. Similarly, Alós et al. (2010) fitted von Bertalanffy growth curves to back-calculated length-at-age data from otoliths for painted comber *Serranus scriba* using a Bayesian approach, using growth parameters specific to the individual. However, these studies did not specifically incorporate year effects, and assumed a direct relationship between otolith increment growth and somatic (body) growth. Weisberg et al. (2010) described additive linear mixed effects models that were empirically used with otolith increment data for Pacific halibut (*Hippoglossus stenolepis*) and smallmouth bass (*Micropterus dolomieu*) respectively, where year and individual effects were treated as random. A modified von Bertalanffy curve (Von Bertalanffy, 1957) was also fit to the data, although it did not perform well with this parameterization, and only age (and not year or individual) effects were estimated. Furthermore, the methods applied by Weisberg et al. (2010) were not simulation-tested, nor were the year effects cross-validated with other local species, as was done in Black (2009).

The main purpose of this study is to develop a mixed effects model using a von Bertalanffy curve – the most commonly used growth model in stock assessment – that incorporates both random individual effects and random year effects, with the aim of obtaining a time-varying index of growth directly from otolith increment data (i.e., the otolith increment data were not converted to length-at-age data). The model was tested in terms of its ability to accurately detect and estimate year effects from simulated otolith increment data, given various samples sizes, life histories, and levels of process and measurement error. To our knowledge, this method (and its parameterization) has not been applied previously for the analysis of otolith band widths for use in estimating climate indices, and has only been made more accessible due to recent developments in nonlinear minimization software.

2. Methods

2.1. Model description

There were three sources of random variation in the model − the year effects, individual within-fish variation, and process error. Year effects could come from any environmental factor or time-varying factor, while individual effects could potentially come from genetic, environmental or behavioral differences. Cohort effects were also considered for the model, but a meta-analysis by Thorson and Minte-Vera, (2016) found they only explained variability of weight-at-age data in about 10 of 91 stocks examined, whereas year effects explained variability in 69 stocks. Process error could come from unknown processes leading to stochasticity and variability in the population dynamics (Rosenberg and Restrepo, 1994). Otolith widths were defined as the distance from the distal dorsal surface to the proximal dorsal surface of an otolith thin section, which is cut along the dorsal-ventral axis, perpendicular to the sulcus, and passing through the focus of each otolith. More details of the data on which this study was based can be found in Black et al. (2005). Otolith width (w) for individual i at year t was modelled using a von Bertalanffy growth function (Von Bertalanffy, 1957):

$$w_{i,t} = \begin{cases} w_{\infty,i,t}(1 - e^{(-K_{i,t}(a_t - a_0))}) + \varepsilon_{inc} & for\ t = 1 \\ w_{i,t-1} + (1 - e^{-K_{i,t}})(w_{\infty,i,t} - w_{i,t-1}) + \varepsilon_{inc} & for\ t > 1 \end{cases} \quad \varepsilon_{\text{inc}} \sim Normal(0, \sigma^2_{inc}) \tag{1a}$$

where w_∞ is the asymptotic width of the otolith along the dorsal-ventral axis, K is the intrinsic growth rate, a_t is the age at year t, a_0 is age for which size is zero, ε_{inc} is the process stochasticity, and σ_{inc} is the standard deviation of the process error. a_0 was not estimated within this model because initial length of the otolith is measured, removing the need for said parameter. Eq. (1a) can also be modified to model otolith growth increments, as opposed to overall widths:

$$w_{i,t} - w_{i,t-1} = (1 - e^{-K_{i,t}})(w_{\infty,i,t} - w_{i,t-1}) + \varepsilon_{inc} \quad \varepsilon_{\text{inc}} \sim Normal(0, \sigma^2_{inc}) \tag{1b}$$

Environmental factors can sometimes have effects on both w_∞ and K, often with inverse effects (Brunel and Dickey-Collas, 2010; Kimura, 2008). Normally-distributed random individual effects $\varepsilon_{w_\infty,i}$ and $\varepsilon_{\text{K},i}$ and year effects ε_t were added to the K and w_∞ parameters, i.e.:

$$\begin{aligned} K_{\text{i,t}} &= K_{base} \cdot e^{\varepsilon_{\text{K},i} + \beta_{\text{K}} \cdot \varepsilon_t} & \varepsilon_{\text{K},i} &\sim Normal(0, \sigma^2_{\text{K}}) \\ w_{\infty,i,t} &= w_{\infty,base} \cdot e^{\varepsilon_{w_\infty,i} + \beta_{w_\infty} \cdot \varepsilon_t} & \varepsilon_{w_\infty,i} &\sim Normal(0, \sigma^2_w) \\ & & \varepsilon_t &\sim Normal(0, 1) \end{aligned} \tag{2}$$

where K_{base} and $w_{\infty,base}$ are the base, mean growth parameters, β_{K} and β_{w_∞} are parameters linking the growth parameters to the year effects, scaling the year effects accordingly, and σ_{K} and σ_w are the standard deviations of the individual effects. The year effects were modelled as a single factor identical between the$K$ and w_∞ parameters – a model that also describes the covariance between the two growth parameters over time (Warton et al., 2015), as determined by the β values. Year effects were presumed to be normally-distributed with a mean of 0 so the mean growth parameters were identifiable, and the population generally following an overall mean growth curve.

2.2. Estimation method

Using Eqs. (1b) and (2), a nonlinear mixed-effects estimation model was developed to quantify individual and temporal variation in otolith growth increments. This model was implemented using Template Model Builder (TMB; Kristensen et al., 2016). β_{K} and β_{w_∞} were freely-estimated, to allow estimation of a positive or negative correlation with the year effects. ε_t was estimated independently (i.e., without an autoregressive component) within this model, under the assumption that ε_t is normal with mean 0 and standard deviation 1. This was to allow for analyses of the year effects to be conducted external to this model procedure, such as fitting AR-1 models to them.

2.3. Fits to data

Several versions of the estimation method were applied to the actual otolith increment data for 66 splitnose rockfish (Black, pers. comm., as

used in his 2005 study). These include a model with no individual nor year variation in growth parameters, a model with only individual effects, a model with only year effects, and a model with both year and individual effects. The selection and validation process for the data is described by Black (2009) and Black et al. (2005). The resultant index of year effects was compared to the published normalized index (Black, 2009; henceforth referred to as the 'published index') using linear regression through the origin.

2.4. Simulation study

The estimation model was tested in terms of the ability to a) detect the presence of year effects, b) correctly estimate year effects given various sample sizes, and c) correctly estimate year effects given different levels of process error. This was accomplished using simulated datasets based on Eqn. (1) and (2), where the true growth model and year effects were known. Growth increments were resampled at the assumed observation error level if the combination of individual effect, year effect, and observation error resulted in negative otolith growth (i.e. when $w_{i,t,observed}$ was greater than w_∞), until the increment was positive. If after 50 re-samples, the increment remained negative, it was set to 0.0000001, as otolith growth continues even when fish growth is negligible, due to the physiochemical process involved in otolith growth (Ashworth et al., 2016).

Simulations were used to examine the sensitivity of the ability to estimate year effects to the amount and the quality of data, and hence to determine how much data are needed to gain an accurate representation of the year effects over 150 years. The number of years was chosen such that it was a longer time period than the longevity of the oldest fish, but short enough that the least oldest fish could theoretically span that time. Three life histories were simulated, based on species that were short-lived and fast-growing (e.g., Pacific sardine *Sardinops sagax*), medium-lived and fast-growing (e.g., petrale sole *Eopsetta jordani*), and long-lived and slow-growing (e.g., splitnose rockfish). Each life history had a unique set of base growth parameters (K_{base} and $w_{\infty,base}$) and maximum age. Each combination of life history, amount of data (number of fish, minimum age of all otoliths as a percentage of the maximum age), and amount of individual and process variance constituted a scenario. 100 datasets were generated for each scenario, and the model was fitted to each dataset, resulting in 100 replicates per scenario. Table 1 shows the values tested for each factor, and every combination of factors that constitutes a scenario. The TMB model and the code for the simulation study can be found on Github (http://github.com/lee-qi/TMB-TVG-growth) for interested readers.

2.4.1. Operating model

100 datasets were generated for each scenario, and the model was fitted to these data. Table 2 lists the parameters used in the data simulation process. Parameter values were obtained by applying an early version of the estimation model to actual otolith data for splitnose rockfish (Table 1; Black, pers. comm.), with the exception of β_K, which was set to −0.001 instead of 1.9E-27, for there to be some time-varying component to K. The K_{base} and $w_{\infty,base}$values for splitnose rockfish were used for the long-lived species, while the values for these parameters for the other life histories were chosen arbitrarily. For each individual fish, its birth year, final age, and the age at which increments first begin were randomly generated from uniform distributions (Table 3), although each individual had at least three growth increments, and increments were bounded to be greater than zero. Year effects ε_t were also randomly generated with an autoregressive lag-1 (AR-1) process, adapted from Thorson et al. (2014):

$$\varepsilon_t = \begin{cases} \rho\varepsilon_{t-1} + \sqrt{1-\rho^2}\,\omega_t & \text{for } t > 1 \\ \omega_t & \text{for } t = 1 \end{cases}$$
$$\omega_t \sim \text{Normal}\left(\frac{-1}{2} \times \frac{1-\rho}{\sqrt{1-\rho^2}}, 1\right) \quad (3)$$

where ρ is the species-specific AR-1 coefficient, and ω_t is independent and identically normally distributed variation for year t, with a standard deviation of 1. The year effects used to generate the data were unique to each replicate, and considered the "true" year effects for that replicate.

2.4.2. Scenarios

Twelve combinations of number of otoliths and minimum age of the otolith (i.e., any otoliths younger than this age were discarded; measured as a proportion of the maximum age) were tested for each of the three life histories, resulting in 36 scenarios (Table 2). These factors were selected due to the confounding natures of the individual and year effects, and their values demonstrate a wide range of sample sizes to identify a sample size sufficient to accurately and precisely estimate the year effects. The estimation method was tested in terms of its ability to correctly identify the presence of year effects (i.e., when $\varepsilon_t = 0$ for all t). One data-poor, one data-moderate, and one data-rich scenario were selected (Table 4) and 100 datasets were simulated with no year effect. Non-informative starting values were used for all parameters of the

Table 1
The parameters used in the model.

Symbol	Description	Value
Fixed Effects		
K_{base}	von Bertalanffy growth coefficient (yr^{-1}; Eq 1)	Varies per life history
$w_{\infty,base}$	Asymptotic length (mm; Eq 1)	Varies per life history
β_K	Multiplicative link parameter to K	−0.001
$\beta_{w\infty}$	Multiplicative link parameter to w_∞	0.008
σ_{inc}	Standard deviation of increment measurements	0.0003
σ_K	Standard deviation of individual effects on K	0.05
σ_w	Standard deviation of individual effects on w_∞	0.03
Random Effects		
$\varepsilon_{K,i}$	Individual effects on K	Normal(0,σ_K)
$\varepsilon_{w\infty,i}$	Individual effects on w_∞	Normal(0,σ_w)
ε_t	Year effects	Normal(0, 1)

Table 2
Description of life histories used and their associated parameters.

Life Histories	Maximum Age (years)	K_{base} (yr^{-1})	$w_{\infty,base}$ (mm)
Short-lived, fast-growing	15	0.2	1
Medium-lived, medium-growing	25	0.1	1.5
Long-lived, slow-growing	100	0.02	2.3

Scenarios Tested	Values
Number of otoliths	20, 50, 100
Minimum age (proportion of maximum age)	0.1, 0.3, 0.5, 0.7

Table 3
The uniform distributions used to generate data.

Randomly-generated data	Minimum Value	Maximum Value
Initial age of otolith (age at which otolith increments start being measured and recorded)	1 year	0.1 of maximum age
Final age of otolith	Minimum age of otolith (Table 2)	Maximum age of otolith (Table 1)
Number of increments	3	Final age – initial age
First year from which increments begin	1	Total years (150) – number of increments

Table 4
Values used in sensitivity analyses.

Scenarios	Life History	Number of fish	Minimum age of otolith (proportion of maximum age)
Data-poor	Short-lived, fast-growing	20	0.1
Data-moderate	Medium-lived, medium-growing	20	0.7
Data-rich	Long-lived, slow-growing	100	0.7

model, except for K_{base} and $w_{\infty,base}$ where the true parameters were used as starting values.

2.4.3. Sensitivity analyses

One data-poor, one data-moderate, and one data-rich scenario (the parameters used to test for detection of non-time-varying growth; Table 4) were selected to examine the sensitivity of the estimation method to process error. The values tested for the process error parameter σ_{inc} were 0.0001, 0.001, 0.01, 0.1, and 0.5. The data-moderate scenario was used to test the sensitivity to σ_{w}values of σ_{K} and For each parameter, the value ranged from 0.01 to 0.10, in 0.03 increments, and each combination of parameters was tested as a scenario.

The medium-lived species (with a minimum otolith age of 0.5 of the maximum age, or 13 years) $\beta_{w_\infty}$was used to test the sensitivity of the estimation method to the values of β_K and For β_{w_∞}, the values tested were 0.001, 0.01, and 0.1, while the values for β_K were set to negative of the same values. Each combination of parameters was tested as a scenario, with varying sample sizes, similar to the data-availability scenarios. In addition, β_K and β_{w_∞} were set to the values obtained from fitting the published index to weight-at-age data in the stock assessment for splitnose rockfish (Gertseva et al., 2009; Lee et al., 2017), in which β_K was found to be 0.13 and β_{w_∞} −0.12.

2.4.4. Performance metrics

Multiplying the estimated two β parameters and ε_t by -1 results in the same maximum likelihood value, which would make it difficult to find the maxim likelihood estimates. This problem can be rectified with an artificial identifiability constraint imposed on the model parameters (e.g., constraining one of the β parameters to be positive), but Stephens (2000) demonstrated that this strategy was not always effective. No constraints were imposed in the estimation phase here. However, this affected the root mean squared error (RMSE) of the estimated year effects. To counter this, RMSE were calculated twice − once based on the estimated year effects ($RMSE = \sum (\widehat{\varepsilon_t} - \varepsilon_t)^2$), and once here each ε_t was multiplied by -1; $RMSE = \sum (\widehat{\varepsilon_t} - (-\varepsilon_t))^2$ − and the minimum of the two recorded. Based on this result, median absolute error ($AE = \hat{\theta} - \theta$) of the year effects was used to evaluate the performance of the estimation method, where $\hat{\theta}$ represents the estimated value (from the estimation method, either multiplied by -1 or not, depending on RMSE) and θ represents the true value (from the operating model).

The correlation between the true time series of year effects and the estimated time series was also investigated using linear regression, with the intercept set to 0. The adjusted R^2 value and the median standard deviation of the error (σ) were used to determine the strength of this correlation. Lee et al. (2017) examined the costs and benefits of incorporating a time-varying growth index in a stock assessment for splitnose rockfish. Using simulation-testing, the authors found that a correlation of 0.77 between the true year effects and the estimated year effects was necessary to reduce the frequency of biased and imprecise population estimates, in conditions where growth was strongly time-varying. The accuracy of the included index was relatively less important when growth was weakly time-varying. Bias in the stock assessment output increased while its precision decreased if the growth index be completely wrong or less than 77% accurate (i.e., not describing true variability in growth). As such, a threshold of 0.77 for the correlation between the true and estimated time series was selected for this study. Median relative errors ($RE = (\hat{\theta} - \theta)/\theta$) of all fixed effect were used to summarize the performance of the estimation method.

3. Results

3.1. Simulation-testing

Scenarios with less informative data (low sample size, minimum age limit, and shorter-lived species) tended to have more runs that failed to converge, where the final gradient of marginal likelihood for each fixed effect was greater than 10^{-6}. This was due in part to there being some years with no data at all (as to be expected in the data-poor situations given a low number of short-lived fish), or the model's inability to find suitable parameters to fit to the data. Additionally, more replicates failed to converge when the parameters relating to the variances of the random effects (i.e., β_K, β_{w_∞}, σ_{inc}, σ_K, and σ_{w}) were high. In a non-simulation scenario, the modeler could tune the estimation method by giving it better starting values. However, this was not feasible given that there were over 8000 replicates in this study. The ability to obtain unbiased and precise estimates of the year effects also depended on the values for the parameters used to generate the data, particularly the parameters relating to the variance of the random effects.

The model generally performed well in terms of its ability to recognize and estimate constant, time-invariant growth across the three data-availability scenarios (Fig. 1). Specifically, the median absolute errors of year effects were estimated near zero in the data-poor and data-moderate scenarios, while β_K and β_{w_∞} were estimated very close to zero in the data-moderate and data-rich scenarios. Given that the true values of the year effects and both β_K and β_{w_∞} were zero in the operating model, the absolute errors thus also show that the estimated values were estimated near zero. Overall, the variances of individual effects were imprecisely estimated, regardless of data availability. Accuracy and precision of the fixed effects increased, and bias decreased, with increased data availability.

The number of otoliths sampled had the largest impact on the estimation method's ability to precisely estimate year effects without bias, with the greatest impact on the short-lived species (Fig. 2). As expected, larger sample sizes led to more accurate and precise estimates of year and fixed effects, and this result holds true for all life histories. Fewer samples (number of otoliths = 20) were required to obtain unbiased year effect estimates for the long-lived species. This might be due to the fact that long-lived species have more growth increments within each otolith, increasing the sample size and degrees of freedom. The estimation method could obtain unbiased and precise estimates of the year effects across all life histories for the largest sample size tested (number of otoliths = 100; Fig. 2). For the long-lived species, the first few and last few years of the time series were the least precisely estimated, which was expected given that there would be more data on the years in the middle of the time series than on the ends. The rate of convergence also increased with longer-lived life history strategies, with a convergence rate of 62–78% for the short-lived species, 69–86% for the medium-lived species, and 85–100% for the long-lived species, as expected given that more data are obtained from otoliths of longer-lived species.

The relationship between estimation performance and the minimum age limit of the otoliths was the most obvious in data-poor scenarios (i.e., when sample sizes were low for the short- and medium-lived species; Fig. 3). The precision of the year effect estimates increased, and bias decreased when only otoliths from older individuals were available. Base growth parameters (K_{base} and $w_{\infty,base}$) were accurately and precisely estimated across scenarios.

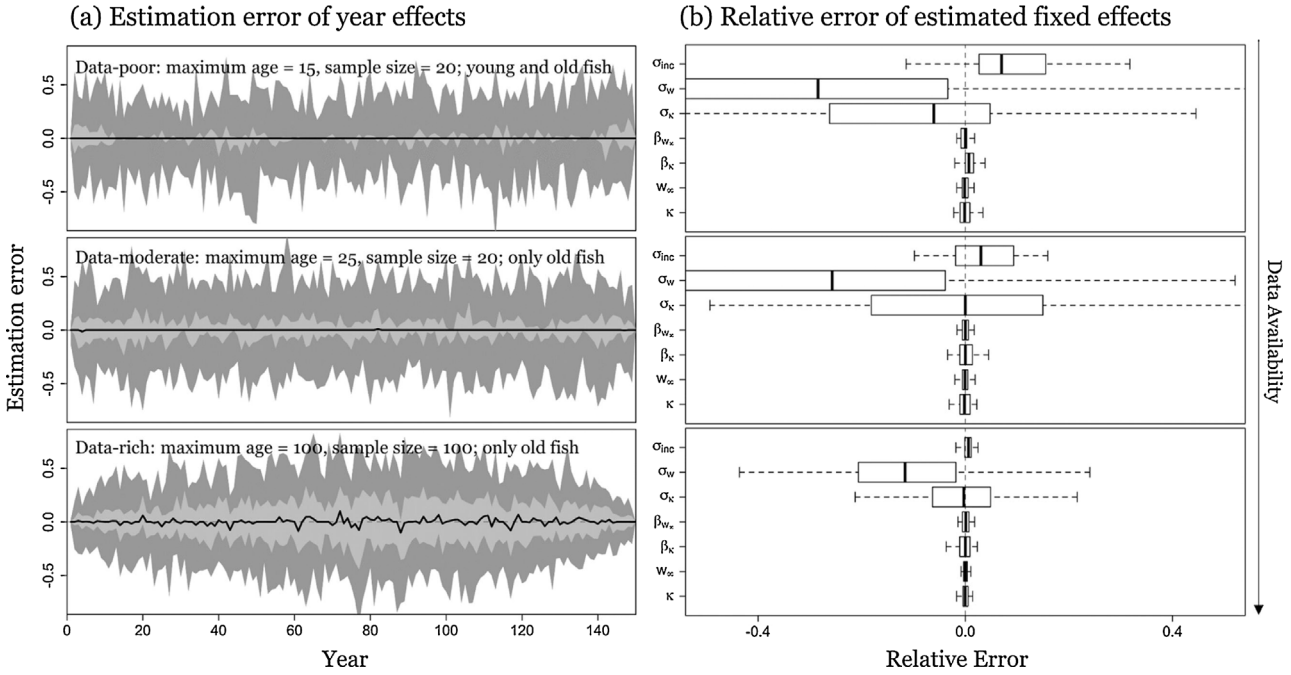

Fig. 1. Summary of results from the scenarios where there was no year effect. Each row represents a life history strategy: top to bottom short-lived to long-lived. Panel (a) shows the absolute errors of estimated year effects. The solid black line represents the median absolute errors, while the light gray and dark gray areas show the 50% and 95% simulation intervals respectively. The dashed black line shows the zero line. Panel (b) shows a boxplot of the relative errors of estimated fixed effects. As the true values of both β parameters are zero, the absolute errors for these parameters are shown. The solid black line represents the median relative error, while boxes show the first and third quantiles. The whiskers show the 95% simulation intervals. The dashed black line is the zero line.

3.2. Sensitivity to error

The ability to accurately estimate the year effects was highly sensitive to the value of σ_{inc} (i.e., the extent of year-individual variation) in all three data-availability scenarios, with higher values for σ_{inc} reducing precision and increasing the bias of year effect and fixed effect estimates (Fig. 4). As σ_{inc} increased, the estimated year effects were increasingly unable to mimic the true year effects, and median R^2 value for the year effects decreased (Fig. 4c). Process error is usually described as the natural variation within a population, driven by abiotic

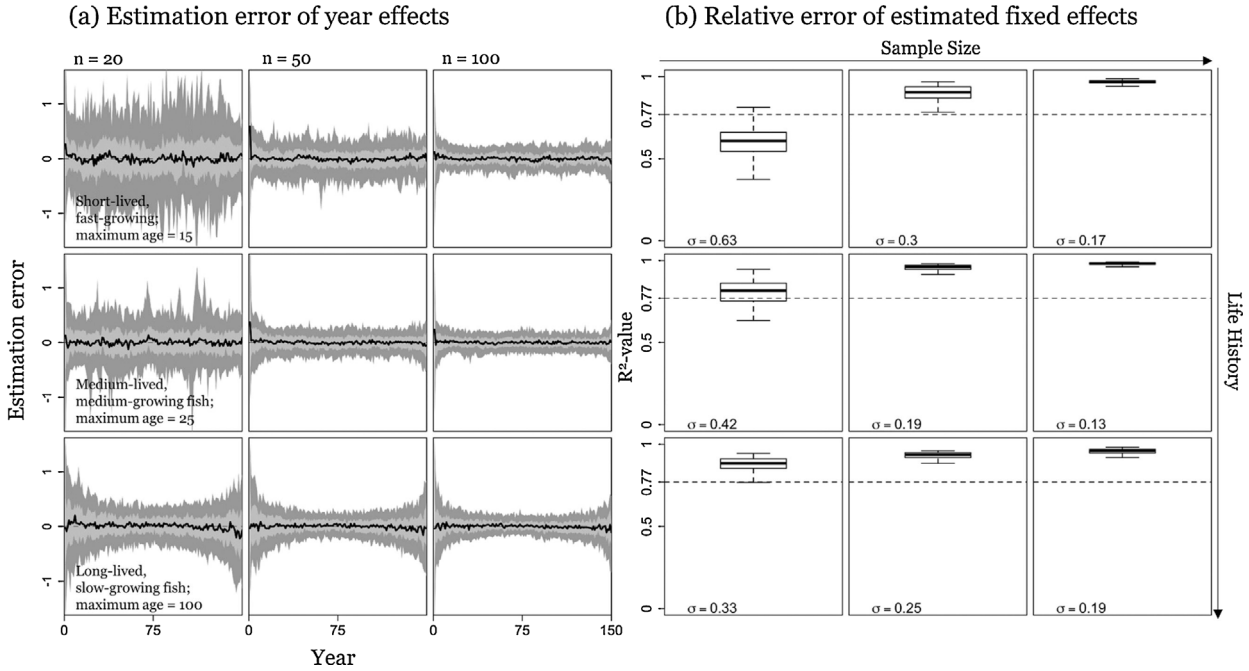

Fig. 2. Summary of results from the sensitivity analysis of year effect estimates to sample size, for a minimum age limit of 0.3 of the maximum age. Each column in a panel represents a sample size, increasing from left to right. Each row represents a life history strategy: top to bottom short-lived to long-lived. Panel (a) shows the absolute errors of estimated year effects. The solid black line represents the median absolute errors, while the light gray and dark gray areas show the 50% and 95% simulation intervals respectively. The dashed black line shows the zero line. Panel (b) shows boxplots of the R^2 value from fitting a linear regression model to test the relationship between the true and the estimated year effects. The solid black line represents the median relative errors, while the boxes show the first and third quantiles. The whiskers show the 95% simulation intervals. The dashed black line is the 0.77 value (obtained from Lee et al., 2017).

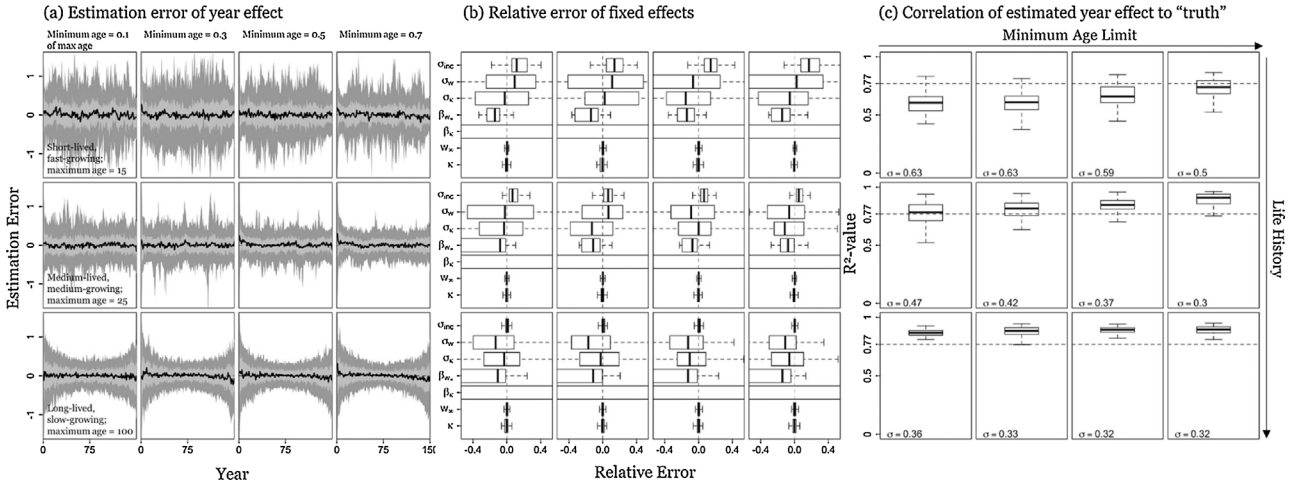

Fig. 3. Summary of results from the sensitivity analysis to minimum age limit for a sample size of 20, the lowest sample size tested. Each row within a panel represents a life history scenario: top to bottom short-lived to long-lived. Each column represents a value of minimum age limit. Panel (a) shows the absolute errors of estimated year effects. The solid black line represents the median absolute errors, while the light gray and dark gray areas show the 50% and 95% simulation intervals respectively. The dashed black line is the zero line. Panel (b) shows boxplots of the relative errors of estimated fixed effects. The solid black line represents the median relative error, while the boxes show the first and third quantiles. The whiskers show the 95% simulation intervals. The dashed black line isthe zero line. Panel (c) shows boxplots of the R^2 value from fitting a linear regression model to test the relationship between the true and the estimated year effects. The dashed black line is the 0.77 value (obtained from Lee et al., 2017).

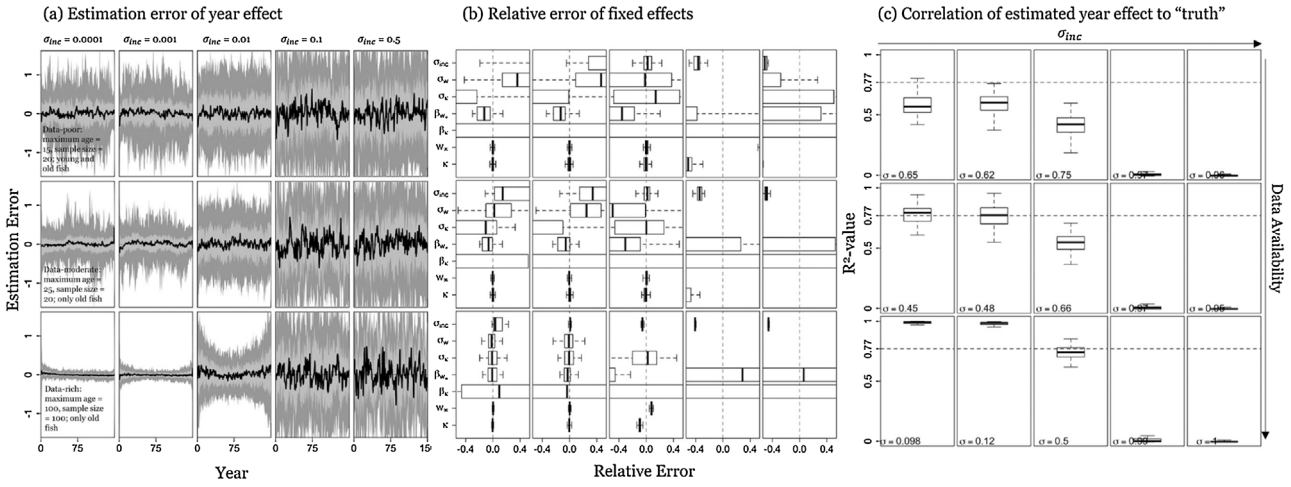

Fig. 4. Summary of results from the sensitivity analysis to the value of σ_{inc}. Each row represents a data-availability scenario: top to bottom data-poor to data-rich. Each column represents a value of σ_{inc}, increasing from left to right. Panel (a) shows the absolute errors of estimated year effects. The solid black line represents the median absolute errors, while the light gray and dark gray areas show the 50% and 95% simulation intervals respectively. The dashed black line is the zero line. Panel (b) shows boxplots of the relative errors of estimated fixed effects. The solid black line represents the median relative error, while the boxes show the first and third quantiles. The whiskers show the 95% simulation intervals. The dashed black line is the zero line. Panel (c) shows boxplots of the R^2 value from fitting a linear regression model to test the relationship between the true and the estimated year effects. The dashed black line is the 0.77 value (obtained from Lee et al., 2017).

or biotic processes not modelled within the population model (Ahrestani et al., 2013). As process error increased, the model increasingly became less able to explain the underlying processes driving the population dynamics, and as such the estimation performance of the year effects decreased, particularly when σ_{inc} was greater than 0.01. This was also likely to have led to the decrease in the number of replicates that converged as σ_{inc} increased.

Increasing individual effects (σ_K and σ_w) reduced the precision and increased bias of year effect and fixed effect estimates (Fig. 5). The rate of convergence increased with increasing values of σ_K, but increasing values of σ_w had no discernable effect on the convergence rate. The value for β_{w_∞} appears to have a larger impact on the accuracy of the year effect estimates than β_K (Fig. 6). Increasing the values of β_{w_∞} also increased the proportion of replicates that converged. At high values of β_{w_∞}, given a sample size of 50 or more, increasing the value of β_K does little to improve the accuracy and precision of the year effect estimates. At low β_{w_∞}, increased β_K values and increasing sample size reduced the bias of year effect estimates, but the sample size had to be greater than 100 (Fig. 6). When β_K and β_{w_∞} were set to stock assessment values (i.e., when the published index was included in the stock assessment model and fit to weight-at-age data; Lee et al., 2017), convergence was low, although the year effect estimates from the converged replicates showed sensitivity to sample size (Fig. 7). The lack of convergence, as mentioned previously, could have been due to the model's sensitivity to uninformative starting values, and improved performance could have been possible given manual tuning.

3.3. Comparison to the index from Black (2009)

The full model that included year and individual effects on K and w_∞ performed best when fitted to actual data for splitnose rockfish, in that it had the lowest AICc value (Table 5). The fits to data for six of the 66 individuals are shown in Fig. 8, and visually it appears that the full model was able to predict observed increment growth for individual

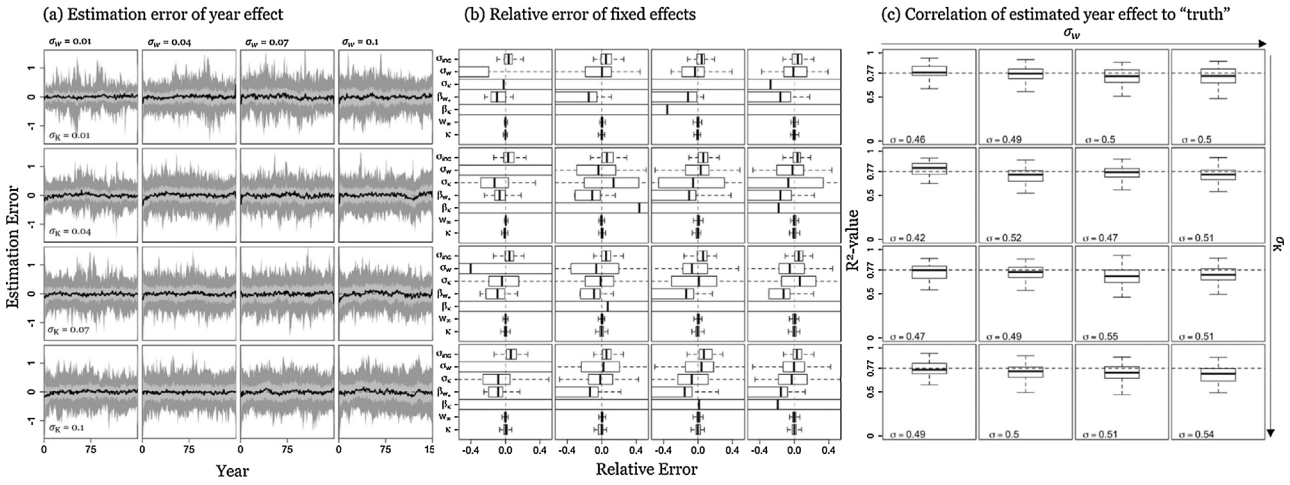

Fig. 5. Summary of results from the sensitivity analysis to the values for σ_w and σ_K, using the data-moderate scenario. Each row represents a value for σ_K, increasing from top to bottom. Each column represents a value of σ_w, increasing from left to right. Panel (a) shows the absolute errors of estimated year effects. The solid black line represents the median absolute errors, while the light gray and dark gray areas show the 50% and 95% simulation intervals respectively. The dashed black line shows the zero line. Panel (b) shows boxplots of the relative errors of estimated fixed effects. The solid black line represents the median relative error, while boxes show the first and third quantiles. The whiskers show the 95% simulation intervals. The dashed black line is the zero line. Panel (c) shows boxplots of the R^2 value from fitting a linear regression model to test the relationship between the true and the estimated year effects. The dashed black line is the 0.77 value (obtained from Lee et al., 2017).

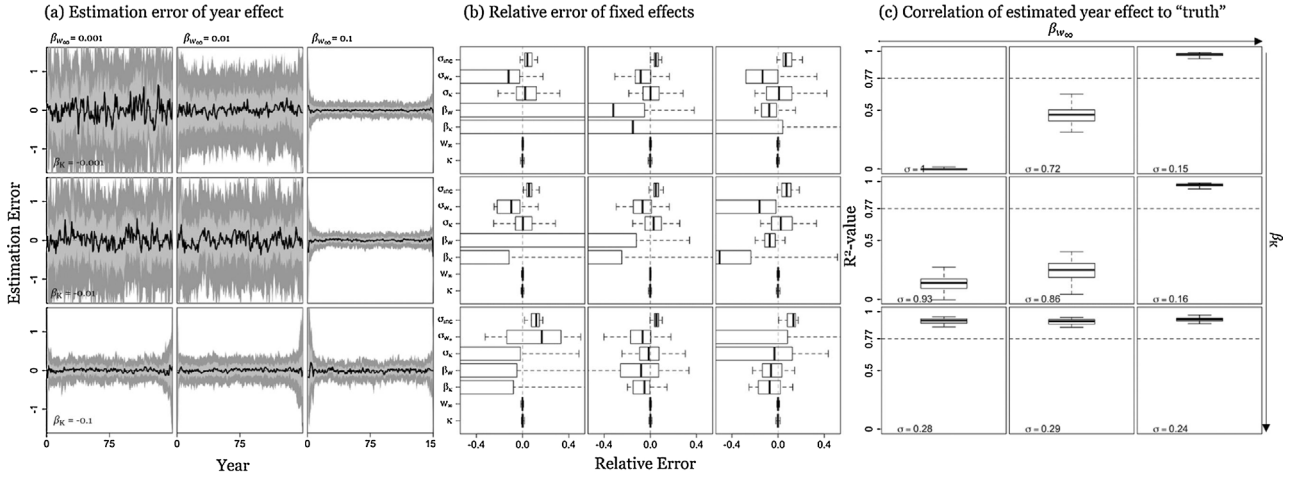

Fig. 6. Summary of results from the sensitivity analysis to the values for β_{w_∞} and β_K, for a sample size of 100. Each row within a panel represents a value for β_K, increasing from top to bottom. Each column represents a value of β_{w_∞}, increasing from left to right. Panel (a) shows the absolute errors of estimated year effects. The solid black line represents the median absolute errors, while the light gray and dark gray areas show the 50% and 95% simulation intervals respectively. The dashed black line is the zero line. Panel (b) shows boxplots of the relative errors of estimated fixed effects. The solid black line represents the median relative error, while boxes show the first and third quantiles. The whiskers show the 95% simulation intervals. The dashed black line is the zero line. Panel (c) shows boxplots of the R^2 value from fitting a linear regression model to test the relationship between the true and the estimated year effects. The dashed black line is the 0.77 value (obtained from Lee et al., 2017).

otoliths with the least error. Residual plots (Supplementary Fig. S1) showed that the model fits the data without bias, although errors were relatively larger at younger ages. Inspection of the correlation matrix for the fixed parameters (Supplementary Table S1) showed a strong correlation between β_K and β_w (R = −0.65), and moderate correlation between$K$ and w_∞ (R = −0.36). The next best model had only individual and no year effects on K (i.e. $\beta_K = 0$), with a ΔAICc value of 6 (Table 5). As β_K was estimated to be very close to 0 in the full model, this low ΔAICc value for the model with no β_K was indicative of the model's convergence at a global value of the likelihood. This low β_K value could have been due to the fact that early years of growth (data which would be most informative to K) were removed from the dataset, which also might explain the larger residuals at younger ages. As a result, model configurations that estimated K as a constant were also tested (i.e., excluding both individual and annual variation in growth K), but not found to fit the data any better (ΔAICc = 672; Table 5). Comparatively, the model with constant growth (i.e., without individual or annual variation in both K and w_∞), performed poorly relative to the other models (ΔAICc = 2262; Table 5) despite having the fewest parameters.

After each model configuration was run, an AR-1 model was fit to the estimated year effects, as was done in Black et al. (2005). The resultant residuals from the AR-1 model (henceforth referred to as the estimated index) were linearly regressed to the published index. The estimated index from the model with time-invariant K (i.e., where the year effects only affected w_∞) was more highly correlated with the published index (R^2 = 0.64) compared with the full model (where year effects affected both K and w_∞; R^2 = 0.57), although both relationships were highly statistically significant ($p < 0.001$; Table 5).

4. Discussion

The proposed approach was able to correctly detect the presence of, and accurately and precisely estimate, year effects given otolith growth

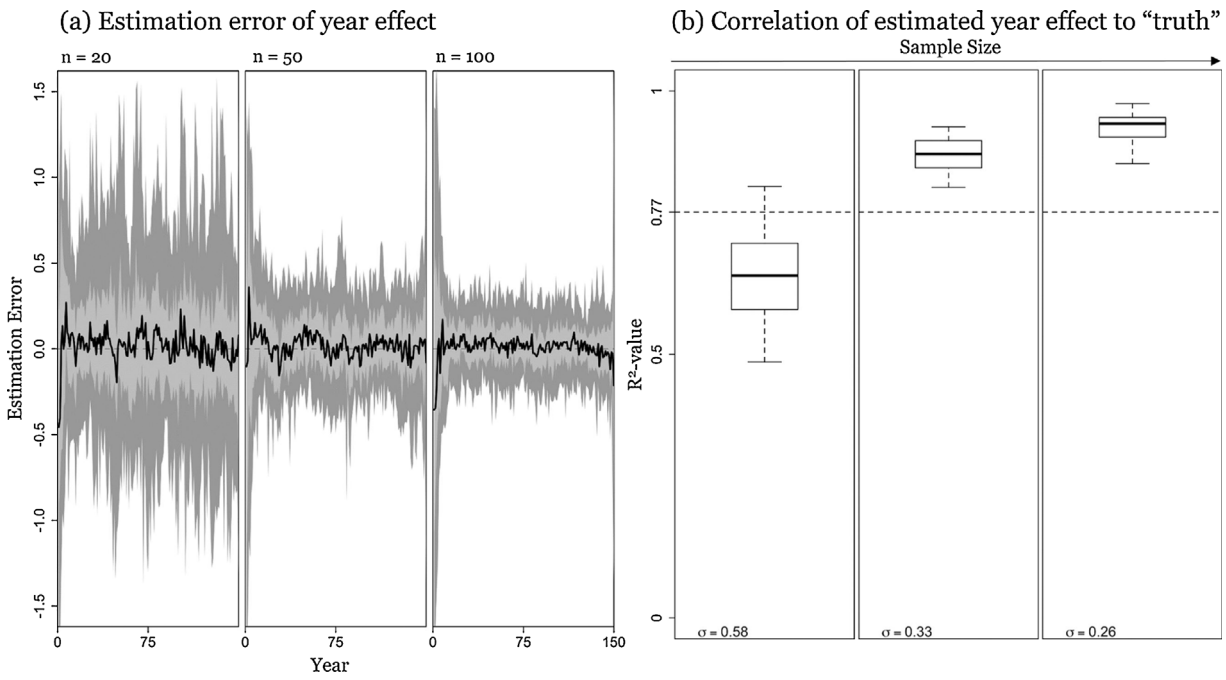

Fig. 7. Summary of results to setting β_w and β_K to the stock assessment values, where the signs are inversed. Each column represents a different sample size. Panel (a) shows the absolute errors of estimated year effects. The solid black line represents the median absolute errors, while the light gray and dark gray areas show the 50% and 95% simulation intervals respectively. The dashed black line is the zero line. Panel (b) shows boxplots of the R^2 value from fitting a linear regression model to test the relationship between the true and the estimated year effects. The dashed black line is the 0.77 value (obtained from Lee et al., 2017).

Table 5
Fixed effect estimates and AICc values for each model configuration fit to the actual data for splitnose rockfish. The R^2 and the estimated variance of error values result from fitting the estimated year effects to the index published by Black (2009).

Model	K_{base}	$w_{\infty,base}$ (mm)	β_K	β_w	σ_{inc}	σ_K	σ_w	R^2 (year effects)	Error (year effects)	AICc	ΔAICc
All effects – individual and year	0.02	2.35	0.46	0.06	0.00	0.50	0.34	0.5725 ($p < 0.001$)	0.6492	−20674	0
No individual or year effects	0.01	2.87	NA	NA	0.01	NA	NA	NA	NA	−18412	2262
Only individual effects	0.01	2.85	NA	NA	4.16E-03	0.43	0.29	NA	NA	−19931	743
Only year effects	0.01	3.05	0.46	−0.24	0.01	NA	NA	0.5453 ($p < 0.001$)	0.6696	−18664	2011
No year effects on K	0.02	2.34	NA	−0.09	3.31E-03	0.50	0.34	0.5454 ($p < 0.001$)	0.6695	−20669	6
Constant K	0.02	2.56	NA	−0.06	4.11E-03	NA	0.16	0.6427 ($p < 0.001$)	0.5935	−20002	672

increment data. Across most scenarios, the model was often unable to unbiasedly and precisely estimate the variance of random effects, which was to be expected as there is often little information on the variability in random effects. The ability of the estimation method to precisely estimate year effects without bias is sensitive to the parameters used to generate the data. By simulation-testing the model, we gain a better understanding of the circumstances and data requirements under which the model performs well at obtaining an unbiased and precise index of time-varying growth. Assuming that a time-varying otolith-growth index approximately scales variations in somatic (body) growth, the residual index could potentially be used to inform growth in stock assessment, and may improve model fit to weight-at-age data. Lee et al. (2017) found that a growth index has to be up to 77% accurate to reduce bias and improve precision in growth estimation in stock assessments, which could be achieved with a sample size of 20 otoliths, if the species in question was long-lived. A sample size of at least 50, or closer to 100, would be ideal, as precise and unbiased year effect estimates would be obtained regardless of life history characteristics. If the β values from fitting the index to weight-at-age data are below 0.3, the index should be included in the assessment anyway, as it is expected to improve overall estimates of spawning stock biomass and recruitment (Lee et al., 2017).

With the estimated year effects from this proposed model, other (such as AR) models can be fit to the index and the residuals used to compare with other indices such as climate indices (Black et al., 2005; Black, 2009). Previous studies have shown that climate can have different effects on the somatic growth than on the otolithic growth of fish, and that otolith growth does not necessarily scale somatic growth linearly (Campana, 1990). For example, somatic growth (fish length) is more dependent on food availability for juvenile King George whiting (*Sillaginodes punctatus*), while changes in otolith growth are more closely related to changes in temperature (Barber and Jenkins, 2001). The latter study, though, was conducted only on juvenile fish for a short period of time (several days). A long-term otolith chronology of mature yellowfin sole *Limanda aspera* was also poorly correlated with individual fish body size, though it was able to capture anomalies in the body mass indices of the entire population (Black et al., 2013). The growth rate parameter estimated in this model does not match the values obtained from the stock assessment of splitnose rockfish ($K = 0.02$ in this study, $K = 0.228$ in Gertseva et al. (2009)), indicating

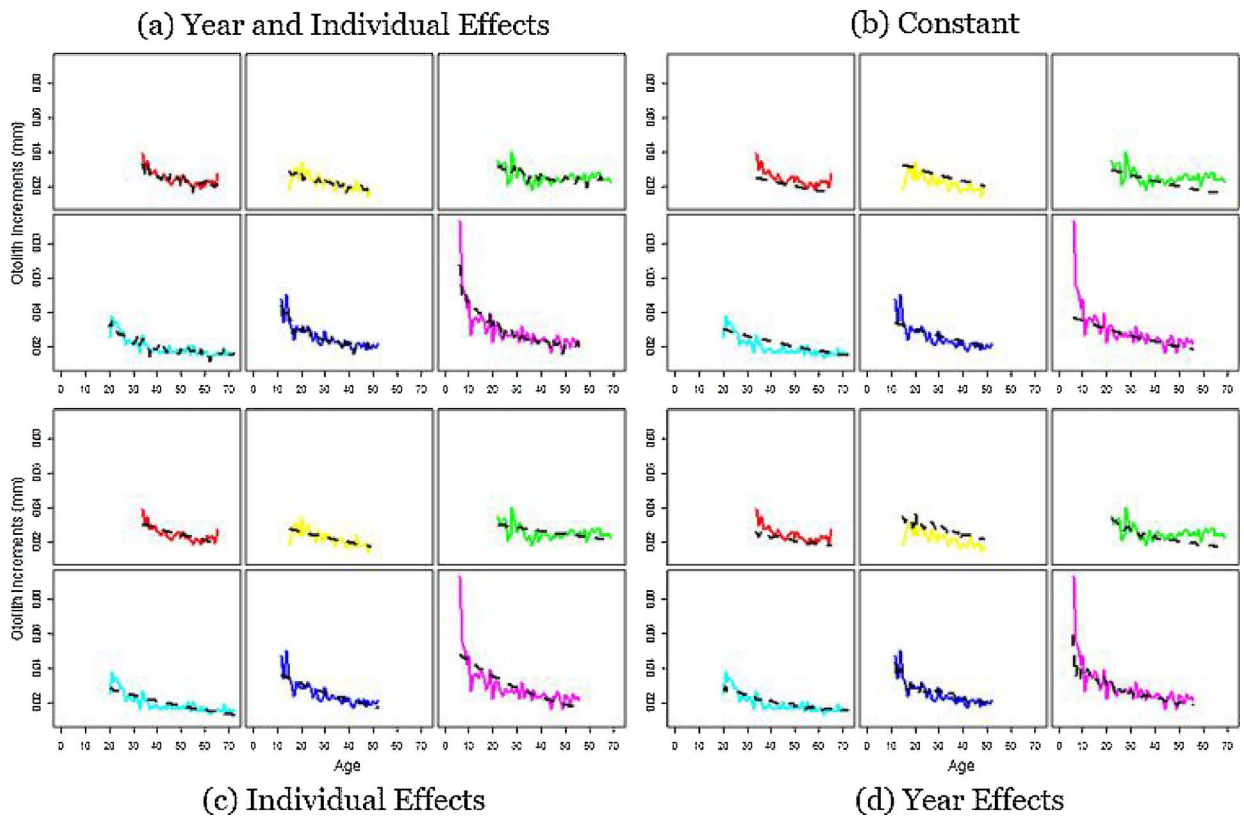

Fig. 8. Model fits to actual otolith increment data for six individual splitnose rockfish, selected out of the total sample size of 66. The solid lines represent the data, with each color representing an individual, while the dashed black line represents model predictions.

that individual otolith growth might be a poor proxy for somatic growth. It would be important to test the sensitivity of a stock assessment model to this growth variation model by combining the derived otolith index to weight-at-age data in a stock assessment to understand its effects on the population's dynamics.

This method was only applied to one set of actual otolith data, and one particular relationship between growth and the environment, and, as in Thorson et al. (2015), the results would only represent populations where these model assumptions are approximately true. The effects of model structure misspecification (e.g., estimating a von Bertalanffy growth function when in fact fish growth follows a Gompertz curve (Gompertz, 1825) or a generic biphasic model (Quince et al., 2008)) were not explored in this study. By misspecifying the growth model, an erroneous index of effects could be estimated, which could then lead to biased management reference points when incorporating said index into assessment models (Lee et al., 2017). The model's ability to detect sexual dimorphic growth (as is the case in splitnose rockfish; Gertseva et al., 2009) was also not tested in this study, although this could presumably be done in future studies by dividing the data set into two components (male and female) and conducting the analysis separately for each sex. Furthermore, this model assumes that age is known without error, when ageing error is a common problem in stock assessments (Punt et al., 2008). The magnitude of measurement error would be very difficult to quantify in this model, but cross-validation of the otoliths, as well as repeated measurements of the otolith widths might be able to minimize this source of error. An example of this process can be found in Black et al. (2005), where the authors cross-dated otoliths by cross-correlating dates of conspicuous (i.e. narrow or wide) increment measurements among samples to validate them. Black (2009) also correlated otolith growth increments among species from the same dates in a similar geographic region, which could be another form of validation. Additionally, due to the covariance in individual variation and annual variation, it could be possible that the model is sensitive to annual or age-specific variation in individual growth (currently modelled as a single time-invariant individual effect), and future studies could estimate whether this component of growth is sufficiently large to impact estimation performance for marine fishes (e.g., Webber and Thorson, 2016). Finally, the model assumes a static relationship between the year effect and both growth parameters (K and w_∞). Variations of the model could include year effects specific to a growth parameter (i.e. one year effect affecting only K and/or another affecting only w_∞), or a functional dependence between the two estimated parameters. However, the data requirements for such information would most likely be substantial.

Applying this approach to other otolith increment data, such as halibut from Weisberg et al. (2010), would increase our understanding of the drivers behind growth in fish. The correlation between otolithic and somatic growth is species-dependent (Ashworth et al., 2016), with this relationship being even more tenuous in tropical fish (Booth, 2014). Hence, this method might not be appropriate fsuch species. As was done in Black (2009) and Coulson et al. (2014), indices obtained from fitting this model to different species within a geographic region can be compared to identify meaningful relationships across species and climate variables. Furthermore, there has been increasing evidence showing spatial variation in growth (e.g., Rahikainen and Stephenson, 2004; Thorson, 2015), and the model could potentially be expanded to include a spatial component.

Black (2009) found that the year effects estimated from splitnose rockfish otoliths, were also correlated with regional climate indices such as the Multivariate El Niño Southern Oscillation Index (MEI) and Pacific Decadal Oscillation (PDO). In light of projected increasing ocean temperatures (Kirtman et al., 2013), it can be expected that climate will continue to impact growth and other aspects of marine fish populations in the future. It is vital that we increase our understanding of time-varying impacts on population dynamics, to reduce model structure uncertainty and to increase forecasting ability. While the proposed

model assumes a constant relationship between climate and fish growth, this might not always be the case (Webber and Thorson, 2016). However, climate and disturbance histories reconstructed using tree-ring data have generally been accurate (e.g., Baker et al., 2005; Esper et al., 2002; Fritts and Arizona, 1991), despite being based on similar assumptions. Furthermore, correlations between otolith widths and tree ring increments have previously been found (Black, 2009; Guyette and Rabeni, 1995), which supports the assumption that the environment will continue affecting fish growth in a similar manner (Morrongiello et al., 2011).

Otoliths contain a wealth of information, and continue to be used an important resource in the management of fisheries (Begg et al., 2005). In this study, we have proposed and simulation-tested a novel method of analyzing otolith data to estimate time-varying growth; using a von Bertalanffy growth curve with random individual and year effects. By applying this method to otolith data, time-varying indices of growth could be obtained and potentially be used in stock assessments. The mechanistic drivers behind time-varying growth still warrant exploration, and the year effects estimated from this model can be used as a first step towards investigating the relationship between climate and growth.

Acknowledgements

This work was supported by NOAA Fisheries and the Environment (FATE) project 13-01. This is the Joint Institute for the Study of the Atmosphere and Ocean (JISAO) NOAA Cooperative Agreement No. NA10OAR4320148, Contribution No. 2017-0126. The authors thank Bryan Black (University of Texas at Austin) for allowing us to use his data. We also thank Timothy Essington (University of Washington), James Thorson (NOAA/NMFS), and two anonymous reviewers for their helpful suggestions and comments on the manuscript.

Appendix A. Supplementary data

Supplementary data associated with this article can be found, in the online version, at https://doi.org/10.1016/j.fishres.2017.12.014.

References

Ahrestani, F.S., Hebblewhite, M., Post, E., 2013. The importance of observation versus process error in analyses of global ungulate populations. Sci. Rep. 3, 3125. http://dx.doi.org/10.1038/srep03125.

Alós, J., Palmer, M., Balle, S., Grau, A.M., Morales-Nin, B., 2010. Individual growth pattern and variability in Serranus scriba: a Bayesian analysis. ICES J. Mar. Sci. 67, 502–512. http://dx.doi.org/10.1093/icesjms/fsp265.

Ashworth, E.C., Hall, N.G., Hesp, S.A., Coulson, P.G., Potter, I.C., 2016. Age and growth rate variation influence the functional relationship between somatic and otolith size. Can. J. Fish. Aquat. Sci. 74, 680–692. http://dx.doi.org/10.1139/cjfas-2015-0471.

Baker, P.J., Bunyavejchewin, S., Oliver, C.D., Ashton, P.S., 2005. Disturbance history and historical stand dynamics of a seasonal tropical forest in western Thailand. Ecol. Monogr. 75, 317–343. http://dx.doi.org/10.1890/04-0488.

Ballagh, A.C., Welch, D., Williams, A.J., Mapleston, A., Tobin, A., Marton, N., 2011. Integrating methods for determining length-at-age to improve growth estimates for two large scombrids. Fish. Bull. 109, 90–100.

Barber, M.C., Jenkins, G.P., 2001. Differential effects of food and temperature lead to decoupling of short-term otolith and somatic growth rates in juvenile King George whiting. J. Fish Biol. 58, 1320–1330. http://dx.doi.org/10.1111/j.1095-8649.2001.tb02289.x.

Begg, G.A., Campana, S.E., Fowler, A.J., Suthers, I.M., 2005. Otolith research and application: current directions in innovation and implementation. Mar. Freshw. Res. 56, 477–483. http://dx.doi.org/10.1071/MF05111.

Black, B.A., Boehlert, G.W., Yoklavich, M.M., 2005. Using tree-ring crossdating techniques to validate annual growth increments in long-lived fishes. Can. J. Fish. Aquat. Sci. 62, 2277–2284. http://dx.doi.org/10.1139/f05-142.

Black, B.A., Matta, M.E., Helser, T.E., Wilderbuer, T.K., 2013. Otolith biochronologies as multidecadal indicators of body size anomalies in yellowfin sole (Limanda aspera). Fish. Oceanogr. 22, 523–532. http://dx.doi.org/10.1111/fog.12036.

Black, B.A., 2009. Climate-driven synchrony across tree, bivalve, and rockfish growth-increment chronologies of the northeast Pacific. Mar. Ecol. Prog. Ser. 378, 37–46. http://dx.doi.org/10.3354/meps07854.

Booth, D.J., 2014. Do otolith increments allow correct inferences about age and growth of coral reef fishes? Coral Reefs 33, 255–258. http://dx.doi.org/10.1007/s00338-013-1105-2.

Brett, J.R., 1979. 10 – environmental factors and growth. In: Hoar, W.S., D.J.R, J.R.B (Eds.), Fish Physiology, Bioenergetics and Growth. Academic Press, pp. 599–675. http://dx.doi.org/10.1016/S1546-5098(08)60033-3.

Brunel, T., Dickey-Collas, M., 2010. Effects of temperature and population density on von Bertalanffy growth parameters in Atlantic herring: a macro-ecological analysis. Mar. Ecol. Prog. Ser. 33, 15–28. http://dx.doi.org/10.3354/meps08491.

Campana, S.E., 1990. How reliable are growth back-calculations based on otoliths? Can. J. Fish. Aquat. Sci. 47, 2219–2227. http://dx.doi.org/10.1139/f90-246.

Coulson, P.G., Black, B.A., Potter, I.C., Hall, N.G., 2014. Sclerochronological studies reveal that patterns of otolith growth of adults of two co-occurring species of Platycephalidae are synchronised by water temperature variations. Mar. Biol. 161, 383–393. http://dx.doi.org/10.1007/s00227-013-2343-0.

Escati-Peñaloza, Parma, G., Orensanz, A.M., (Lobo), J.M., 2010. Analysis of longitudinal growth increment data using mixed-effects models: individual and spatial variability in a clam. Fish. Res. 105, 91–101. http://dx.doi.org/10.1016/j.fishres.2010.03.007.

Esper, J., Cook, E.R., Schweingruber, F.H., 2002. Low-frequency signals in long tree-ring chronologies for reconstructing past temperature variability. Science 295, 2250–2253. http://dx.doi.org/10.1126/science.1066208.

Essington, T.E., Kitchell, J.F., Walters, C.J., 2001. The von Bertalanffy growth function, bioenergetics, and the consumption rates of fish. Can. J. Fish. Aquat. Sci. 58, 2129–2138.

Eveson, J.P., Million, J., Sardenne, F., Le Croizier, G., 2015. Estimating growth of tropical tunas in the Indian Ocean using tag-recapture data and otolith-based age estimates. Fish. Res. 163, 58–68. http://dx.doi.org/10.1016/j.fishres.2014.05.016. (IO Tuna tagging).

Fritts, Arizona, H.C.U., 1991. Reconstructing Large-scale Climatic Patterns from Tree-ring Data.

Gertseva, V.V., Cope, J.M., Pearson, D.E., 2009. Status of the US Splitnose Rockfish (Sebastes Diploproa) Resource in 2009, Status of the Pacific Coast Groundfish Fishery Through 2009 and Recommended Acceptable Biological Catches for 2011/2012: Stock Assessment and Fishery Evaluation, 2009. Northwest Fisheries Science Center, NOAA Fisheries, Portland, OR.

Gertseva, V., Cope, J., Matson, S., 2010. Growth variability in the splitnose rockfish Sebastes diploproa of the northeast Pacific Ocean: pattern revisited. Mar. Ecol. Prog. Ser. 413, 125–136. http://dx.doi.org/10.3354/meps08719.

Gompertz, B., 1825. On the nature of the function expressive of the law of human mortality, and on a new mode of determining the value of life contingencies. Philos. Trans. R. Soc. Lond. 115, 513–583.

Guyette, R.P., Rabeni, C.F., 1995. Climate response among growth increments of fish and trees. Oecologia 104, 272–279.

Helser, T.E., Lai, H.-L., 2004. A Bayesian hierarchical meta-analysis of fish growth: with an example for North American largemouth bass, Micropterus salmoides. Ecol. Model. 178, 399–416. http://dx.doi.org/10.1016/j.ecolmodel.2004.02.013.

Helser, T.E., Stewart, I.J., Lai, H.-L., 2007. A Bayesian hierarchical meta-analysis of growth for the genus Sebastes in the eastern Pacific Ocean. Can. J. Fish. Aquat. Sci. 64, 470–485. http://dx.doi.org/10.1139/f07-024.

Kimura, D.K., 2008. Extending the von Bertalanffy growth model using explanatory variables. Can. J. Fish. Aquat. Sci. 65, 1879–1891. http://dx.doi.org/10.1139/F08-091.

Kirtman, B., Power, S.B., Adedoyin, A.J., Boer, G.J., Bojariu, R., Camilloni, I., Doblas-Reyes, F., Fiore, A.M., Kimoto, M., Meehl, G., Prather, M., Sarr, A., Schar, C., Sutton, R., van Oldenborgh, G.J., Vecchi, G., Wang, H.-J., 2013. Chapter 11 – near-term climate change: projections and predictability. In: IPCC (Ed.), Climate Change 2013: The Physical Science Basis. IPCC Working Group I Contribution to AR5. Cambridge University Press, Cambridge.

Kristensen, K., Nielsen, A., Berg, C.W., Skaug, H.J., Bell, B.M., 2016. TMB: automatic differentiation and laplace approximation. J. Stat. Softw. 70, 1–21. http://dx.doi.org/10.18637/jss.v070. i05.

López-Abellán, L.J., Santamaría, M.T.G., González, J.F., 2008. Approach to ageing and growth back-calculation based on the otolith of the southern boarfish Pseudopentaceros richardsoni (Smith, 1844) from the south-west Indian Ocean seamounts. Mar. Freshw. Res. 59, 269–278. http://dx.doi.org/10.1071/MF07131.

Lee, Q., Thorson, J.T., Gertseva, V.V., Punt, A.E., 2017. The benefits and risks of incorporating climate-driven growth variation into stock assessment models, with application to Splitnose Rockfish (Sebastes diploproa). ICES J. Mar. Sci. http://dx.doi.org/10.1093/icesjms/fsx147.

Liang, K.-Y., Zeger, S.L., 1986. Longitudinal data analysis using generalized linear models. Biometrika 73, 13–22. http://dx.doi.org/10.2307/2336267.

Lorenzen, K., 2016. Toward a new paradigm for growth modeling in fisheries stock assessments: embracing plasticity and its consequences. Fish. Res. 180, 4–22. http://dx.doi.org/10.1016/j.fishres.2016.01.006.

Morrongiello, J.R., Crook, D.A., King, A.J., Ramsey, D.S.L., Brown, P., 2011. Impacts of drought and predicted effects of climate change on fish growth in temperate Australian lakes. Glob. Change Biol. 17, 745–755. http://dx.doi.org/10.1111/j.1365-2486.2010.02259.x.

Palmer, M.J., Phillips, B.F., Smith, G.T., 1991. Application of nonlinear models with random coefficients to growth data. Biometrics 47, 623–635. http://dx.doi.org/10.2307/2532151.

Pannella, G., 1980. Growth patterns in fish sagittae. Skeletal Growth of Aquatic Organisms. Biological Records of Environmental Change, Topics in Geobiology. Springer US, pp. 519–560.

Pilling, G.M., Kirkwood, G.P., Walker, S.G., 2002. An improved method for estimating individual growth variability in fish, and the correlation between von Bertalanffy growth parameters. Can. J. Fish. Aquat. Sci. 59, 424–432. http://dx.doi.org/10.1139/f02-022.

Pinheiro, J.C., Bates, D.M., 2000. Linear mixed-effects models: basic concepts and examples. Mixed-Effects Models in S and S-PLUS, Statistics and Computing. Springer New York, pp. 3–56. http://dx.doi.org/10.1007/0-387-22747-4_1.

Punt, A.E., Smith, D.C., KrusicGolub, K., Robertson, S., 2008. Quantifying age-reading error for use in fisheries stock assessments, with application to species in Australia's southern and eastern scalefish and shark fishery. Can. J. Fish. Aquat. Sci. 65, 1991–2005. http://dx.doi.org/10.1139/F08-111.

Quince, C., Abrams, P.A., Shuter, B.J., Lester, N.P., 2008. Biphasic growth in fish I: theoretical foundations. J. Theor. Biol. 254, 197–206. http://dx.doi.org/10.1016/j.jtbi.2008.05.029.

Rahikainen, M., Stephenson, R.L., 2004. Consequences of growth variation in northern Baltic herring for assessment and management. ICES J. Mar. Sci. 61, 338–350. http://dx.doi.org/10.1016/j.icesjms.2004.02.005.

Rosenberg, A.A., Restrepo, V.R., 1994. Uncertainty and risk evaluation in stock assessment advice for U.S. marine fisheries. Can. J. Fish. Aquat. Sci. 51, 2715–2720. http://dx.doi.org/10.1139/f94-271.

Stawitz, C.C., Essington, T.E., Branch, T.A., Haltuch, M.A., Hollowed, A.B., Spencer, P.D., 2015. A state-space approach for detecting growth variation and application to North Pacific groundfish. Can. J. Fish. Aquat. Sci. 72, 1316–1328. http://dx.doi.org/10.1139/cjfas-2014-0558.

Stephens, M., 2000. Dealing with label switching in mixture models. J. R. Stat. Soc. Ser. B Stat. Methodol. 62, 795–809. http://dx.doi.org/10.1111/1467-9868.00265.

Strom, A., Francis, R.C., Mantua, N.J., Miles, E.L., Peterson, D.L., 2004. North Pacific climate recorded in growth rings of geoduck clams: a new tool for paleoenvironmental reconstruction. Geophys. Res. Lett. 31, L06206. http://dx.doi.org/10.1029/2004GL019440.

Thorson, J.T., Minte-Vera, C.V., 2016. Relative magnitude of cohort, age, and year effects on size at age of exploited marine fishes. Fish. Res. 180, 45–53. http://dx.doi.org/10.1016/j.fishres.2014.11.016.

Thorson, J.T., Jensen, O.P., Zipkin, E.F., 2014. How variable is recruitment for exploited marine fishes? A hierarchical model for testing life history theory. Can. J. Fish. Aquat. Sci. 71, 973–983. http://dx.doi.org/10.1139/cjfas-2013-0645.

Thorson, J.T., Monnahan, C.C., Cope, J.M., 2015. The potential impact of time-variation in vital rates on fisheries management targets for marine fishes. Fish. Res. 169, 8–17. http://dx.doi.org/10.1016/j.fishres.2015.04.007.

Thorson, J.T., 2015. Spatio-temporal variation in fish condition is not consistently explained by density, temperature, or season for California current groundfishes. Mar. Ecol. Prog. Ser. 526, 101–112.

Von Bertalanffy, L., 1957. Quantitative laws in metabolism and growth. Q. Rev. Biol. 32, 217–231.

Warton, D.I., Blanchet, F.G., O'Hara, R.B., Ovaskainen, O., Taskinen, S., Walker, S.C., Hui, F.K.C., 2015. So many variables: joint modeling in community ecology. Trends Ecol. Evol. 30, 766–779. http://dx.doi.org/10.1016/j.tree.2015.09.007.

Weatherley, A.H., 1990. Approaches to understanding fish growth. Trans. Am. Fish. Soc. 119, 662–672. http://dx.doi.org/10.1577/1548-8659(1990)119<0662:ATUFG>2.3.CO;2.

Webber, D.N., Thorson, J.T., 2016. Variation in growth among individuals and over time: a case study and simulation experiment involving tagged Antarctic toothfish. Fish. Res. 180, 67–76. http://dx.doi.org/10.1016/j.fishres.2015.08.016.

Weisberg, S., 1993. Using Hard-part Increment Data to Estimate Age and Environmental Effects. Can. J. Fish. Aquat. Sci. 50, 1229–1237. http://dx.doi.org/10.1139/f93-139.

Weisberg, S., Spangler, G., Richmond, L.S., 2010. Mixed effects models for fish growth. Can. J. Fish. Aquat. Sci. 67, 269–277. http://dx.doi.org/10.1139/F09-181.

Wishart, J., 1938. Growth-rate determinations in nutrition studies with the bacon pig, and their analysis. Biometrika 30, 16–28. http://dx.doi.org/10.2307/2332221.

Xu, H., Sun, Y., Wang, X., Fu, Y., Dong, Y., Li, Y., 2014. Nonlinear mixed-effects (NLME) diameter growth models for individual china-fir (Cunninghamia lanceolata) trees in southeast China. PLoS One 9. http://dx.doi.org/10.1371/journal.pone.0104012.

Zeger, S.L., Liang, K.-Y., 1986. Longitudinal data analysis for discrete and continuous outcomes. Biometrics 42, 121–130. http://dx.doi.org/10.2307/2531248.

Zhang, Z., Lessard, J., Campbell, A., 2009. Use of Bayesian hierarchical models to estimate northern abalone, Haliotis kamtschatkana, growth parameters from tag-recapture data. Fish. Res. 95, 289–295. http://dx.doi.org/10.1016/j.fishres.2008.09.035.

Zhu, X., Tallman, R.F., Howland, K.L., Carmichael, T.J., 2016. Modeling spatiotemporal variabilities of length-at-age growth characteristics for slow-growing subarctic populations of Lake Whitefish, using hierarchical Bayesian statistics. J. Gt. Lakes Res. 42, 308–318. http://dx.doi.org/10.1016/j.jglr.2015.08.013.